NRIAG JOURNAL OF ASTRONOMY AND GEOPHYSICS
2021, VOL. 10, NO. 1, 347–360
https://doi.org/10.1080/20909977.2021.1938893

Structural interpretation of magnetic and satellite remotely sensed data of Osun State, Southwestern, Nigeria

Adebiyi S. Adebayo[a], Emmanuel A. Ariyibi[b], Oluwaseyi A. Dasho[b,c], Charles I. Adenika[b] and Emmanuel O. Olagunju[d]

[a]Department of Physics, University of Medical Sciences, Ondo, Nigeria; [b]Department of Physics and Engineering Physics, Obafemi Awolowo University, Ile-Ife, Nigeria; [c]Department of Physical Sciences, Dominion University Ibadan, Oyo, Nigeria; [d]Department of Physics, Afe Babalola University, Ado-Ekiti, Nigeria

ABSTRACT

This study delineates surface and subsurface structural features in the hard rock terrain of Osun State using magnetic data and satellite remote sensing imageries. To achieve this aim, several image enhancement methods were applied to the magnetic data and satellite remotely sensed imageries to improve visualization and interpretation. The subsurface lineaments were detected and traced out from the maxima of Horizontal Gradient Magnitude, peaks of Analytical Signal Magnitude, and an Euler solution of Osun state. The magnetic lineament map reveals that the structural trend in the area is dominant by NE-SW and NNE-SSW. These structural trends were found to be consistent with the regional tectonics of the Southwest Basement of Nigeria. The NE-SW is the most conspicuous structural trend in the study area. The satellite imageries depict a characteristics feature of the occurrence of underlying structures in the basement complex of Osun State. The major lineament trends delineated in the composite surface lineament map are the NE-SW, NNE-SSW, and ENE-WSW directions. The 2.5 D model across the unmapped lineaments confirmed the existence of a thin dyke's characteristic of fracture/fault in a typical basement complex terrain. The derived lineaments may serve as a reference for future geological and structural mapping.

ARTICLE HISTORY
Received 10 October 2019
Revised 22 April 2021
Accepted 1 June 2021

KEYWORDS
Airborne magnetic data; satellite remote sensing; faults; lineaments

1. Introduction

Significant parts of Southwestern Nigeria are underlain by basement complex rocks which are associated with high lineaments density. Delineation of these lineaments on a regional scale through the ground geophysical survey can be time-consuming and laborious. However, airborne magnetic and satellite remote data provide a rapid and cost-effective method for delineating subsurface and surface geologic frameworks. The knowledge of the structural setting and subsurface sequence of an area is crucial in hazard assessment and natural resource exploration. Infrastructures sited on geological structures such as fault are prone to high structural damages. Mapping of these fault zones is economically important as it can serve as a reservoir for the accumulation of hydrothermal fluid (Oelkers et al. 2009), hydrocarbons (Wu et al. 2014; Jiang et al. 2018), groundwater (Dasho et al. 2017; Oyeyemi and Aizebeokhai 2018; Olorunfemi and Oni 2019), base and precious metal ore deposits, and geothermal energy (Elhag and Bahrawi 2014). Geological mapping for geologic structures is difficult in areas with subdued surface relief, limited rock outcrops, or where the faults are mostly buried beneath large accumulations of sediment. However, geophysical methods such as Ground Penetrating Radar, Magnetic, Gravity, Electromagnetic and Seismic methods provide a means of obtaining subsurface information in areas with partial/complete cover by alluvium, colluvium and vegetation, and these methods have been used by Boucher 1995; Masoud et al. 2007 to map geologic features such as intrusive rocks, folds, and faults. Also, remote-sensing techniques involving the use of multispectral and optical data have been used to discriminate different lithology and lineaments (Masoud and Koike 2011; Bahiru and Woldai 2016; Dasho et al. 2017; Adebayo 2018). This paper identifies surface and subsurface structural features in Osun State using airborne magnetic data and satellite remotely sensed data, also investigated the existence of some of the suspected faults using a ground magnetic survey, which measures the magnetic amplitude at discrete points across the suspected faults. This investigation is crucial to the understanding of the tectonic framework of Osun state and also to validate the existence of some of the suspected faults, which subsequently can be used as a reference in future geological and structural mapping.

2. Description of the study area

Osun State (the study area) is situated in southwestern Nigeria (Figure 1), between latitudes 7° 00′ N to 8° 15′

CONTACT Adebiyi S. Adebayo adebayo_adebiyi08@yahoo.com Department of Physics, University of Medical Sciences, Ondo, Nigeria

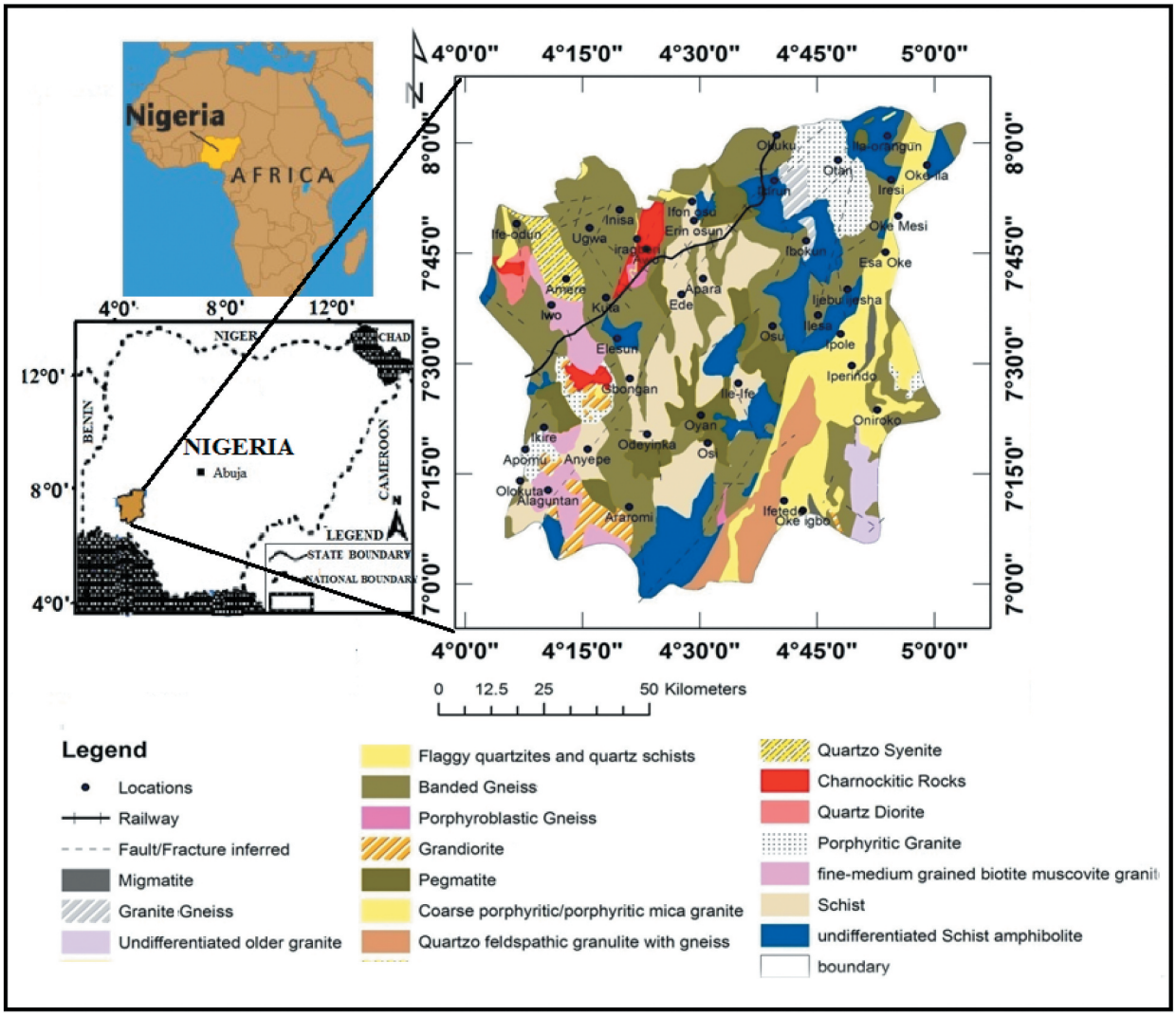

Figure 1. Location of the study area shown with geological map of Osun State (after NGSA 2006).

N and longitudes 4° 00′ E to 5° 15′ E. Climatically, Osun State located within the tropical climatic region characterised by alternately dry and wet seasons. The dry season is usually experienced in November to March while the wet season is experienced from April to October (Adetoyinbo et al. 2010). The daily average temperature of the study area ranges from 20°C (cold day) to 35°C (hot day). Geologically, the southwest basement complex of Nigeria is composed of six dominant rock groups (Rahaman 1976). The Migmatite-Gneiss Complex is the oldest and most widespread; the Slightly Migmatised to non migmatised Para-Schists and Meta Igneous rocks are known to conceal valuable economic mineral deposits; Charnockitic rocks are significant petrological units in the Precambrian basement complex of Nigeria. The rocks comprised of two basic varieties: bauchite and charnockites; the Older Granites were first recognised from the Younger Granites by Falconer (1911). They extend in size from plutons to batholiths. The Older Granite is fractured, faulted, and jointed; Metamorphosed to non-metamorphosed Calc-Alkaline Volcanics and Hypabyssal Rocks, the rocks are often related to faults that controlled their emplacement.

3. Materials, methods and initial data appraisal

3.1. Materials

In this study, several types of datasets were used. They include aeromagnetic datasets (covering Iwo, Ilesha, Ondo, Ilorin, Ado Ekiti, Osi and Apomu sheets), ground magnetic data, Landsat-7 ETM+ scenes (P190R54, P190R55, P191R54, and P191R55), Digital Elevation Map and geological map of the study area.

3.2. Airborne magnetic data and initial data appraisal

The aeromagnetic datasets used in this study were acquired by Fugro Airborne Surveys for the Nigerian Geological Survey Agency (NGSA),

a highly sensitive 3x Scintrex C53 Caesium Vapour magnetometer was used for the survey. The data acquisition was carried out at a flight height of 80 m, flight line spacing of 0.5 km and tie-line spacing of 2 km, the flight line, and tie line direction are NW-SE and NE-SW, respectively. The removal of the non-crustal effects from the acquired aeromagnetic data was done through the removal of the International Geomagnetic Reference Field (IGRF). The airborne magnetic datasets of the study area were gridded to an equal cell size of 100 m using a minimum curvature method (Briggs 1974; Webring 1981). To convert the magnetic intensity data acquired at different magnetic field inclinations to what they would be with zero inducing field inclination, the TMI map (Figure 2(a)) was transformed to Reduction-to-Equator (RTE) map (Figure 2(b)), this step is considered necessary in low magnetic latitude area like the study area (Keating and Zerbo 1996). To reveal abrupt changes in magnetisation and highlight anomaly pattern discontinuities that may suggest source contacts/faults, Horizontal Gradient Magnitude (HGM) was computed (Figure 3(a)) using Equation (1), where T is the magnetic field in the x and y directions

$$\mathrm{HGM}(x,y)=\sqrt{\left(\frac{\partial T}{\partial x}\right)^2+\left(\frac{\partial T}{\partial y}\right)^2} \tag{1}$$

HGM works on the assumption of vertical source magnetisations and regional magnetic field, and thus generate apparent contacts, which are continuous and linear (Phillips 2000). Also, Analytical Signal Magnitude (Figure 3(b)) was calculated using Equation (2) (MacLeod et al. 1993).

$$|A(x,y,z)|=\sqrt{\left(\frac{\partial T}{\partial x}\right)^2+\left(\frac{\partial T}{\partial y}\right)^2+\left(\frac{\partial T}{\partial z}\right)^2} \tag{2}$$

Euler deconvolution (Figure 4) was calculated using the homogeneity Equation (3) to estimates of source position and depth for different targets (contacts, dyke, sphere cylinder).

$$(x-x_O)\frac{\partial T}{\partial x}+(y-y_O)\frac{\partial T}{\partial y}++(z-z_O)\frac{\partial T}{\partial z}=N(B-T) \tag{3}$$

where x_O,y_O and z_O are the locations of the magnetic source which creates the total magnetic field T estimated at xyz directions, N is the Structural Index and B is the regional value of the total magnetic field. The resulting maps were combined to form a composite magnetic lineament map of the study area.

3.3. Ground magnetic surveys and initial data appraisal

Ground magnetic surveys were conducted and measurements were taken at 10 m interval across two preciously unmapped lineaments delineated by airborne magnetic data. The length of the four traverses varies from 1.2 to 2.2 km. Base stations were established outside each traverse and repeated ground magnetic readings were carried out at these stations prior to and after magnetic readings were made on the traverses, respectively. The impact of a variety of the earth's magnetic field with time due to the earth's revolution to the solar wind was corrected by subtracting the base station measurement from the traverse station measurement at a synchronised time. The subsequent residual total field data were treated using three points running average filtering to wipe out spikes. Noise as a result of secular change/epoch was viewed as irrelevant because steady measurements were taken at the base station each hour. The magnetic data along the four profiles were qualitatively and quantitatively interpreted by a method involving 2.5D inversing using WingLink software. Several models were tried until a geologically plausible magnetic inversion model was accomplished.

3.4. Landsat-7 ETM+ data and initial data appraisal

To map the surface geological lineaments, four scenes of Landsat-7 ETM+ (Paths/Rows 190/54, 190/55, 191/54, and 191/55) with 0% cloud cover were downloaded from http://glovis.usgs.gov/ website. These images were mosaicked into a seamless single image. Several digital pre-processing techniques were applied to the remotely sensed image to increase the sharpness and clarity of the image to obtain more reliable information. This processing includes Spectral enhancement used to determine the best bands combination for lineament extraction. Out of the 20 possible combinations of original image bands tested, five gives reasonable enhancements for false colour composites (FCC) in RGB mode. Of these five, Bands 742 were the most satisfactory using Optimum Index Factor (OIF), drainage, and topography as criteria for selection. The bands with the highest Optimum Index Factor contain the highest spectral information (Dasho et al. 2017). The panchromatic band with 15 m resolution was fused with the 30 m FCC image for improved resolution; this process is known as resolution enhancement. Radiometric enhancement was carried out on the pan-sharpened FCC image to increase the visual contrast of the raster display. The image was edge enhanced to accentuate the comparative difference between a cell's Values and its neighbour's, to highlight boundaries

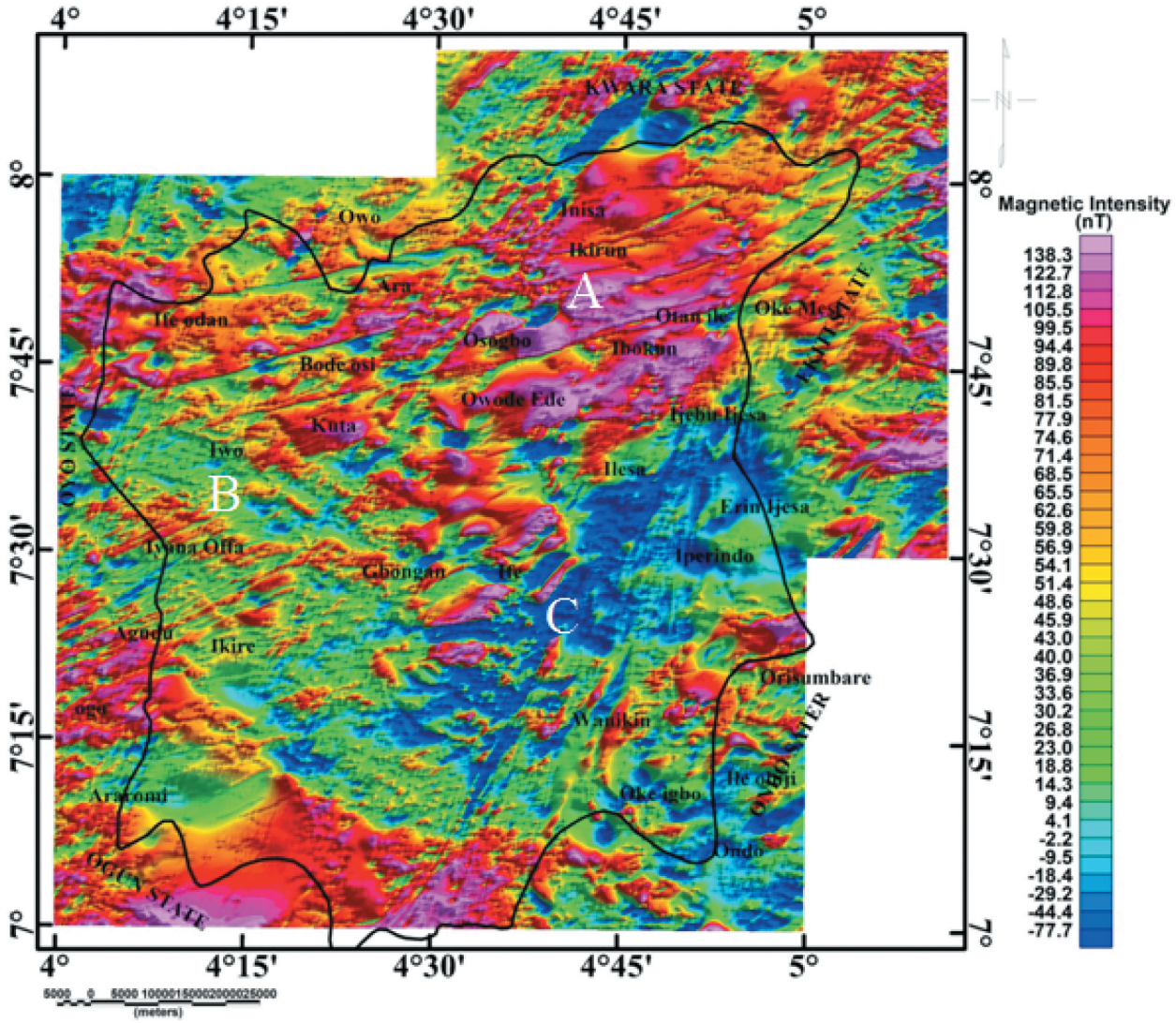

Figure 2. (a) Total magnetic intensity (TMI) Map of Osun State. (b) Reduced to the equator (RTE) Map of the total magnetic intensity (TMI) Map of Osun State.

between features. The enhanced Landsat-7 ETM+ image was imported into the PCI Geomatica 2014 software which uses a robust Canny edge detection algorithm for automatic lineament extraction. The algorithm of PCI Geomatica comprises edge detection, thresholding and curve Extraction steps (Geomatica 2014). The adopted parameters setting used in this work for lineament extraction were presented in Table 1. The non-geological lineaments were subsequently removed by overlaying the lineaments on the high-resolution Google Earth image at zoomed.

3.5. ASTER data and initial data appraisal

The second satellite image used in this study is the ASTER DEM with 90-m spatial resolution. The Digital Elevation Model (DEM) was extracted from the ASTER data to discern and extract surface geological lineaments. A depressionless DEM of the study area was produced by the removal of sinks (peaks) using ArcGIS 10.1. The corrected image was then used to produce a shaded relief map. The shaded relief map was calculated on the map using varied azimuth directions (0°, 45°, 90°, 135°, 180°, 225°, 270°, 315°, 360°) with the sun angle of 30° and scaling factor $9.12x10^{-6}$. Automatic lineament extraction was performed on the shaded relief map to generate lineament using the algorithm of PCI Geomatica and the adopted parameters setting as contained in Table 1.

4. Results and discussion

4.1. Qualitative interpretation of aeromagnetic map

The first step examined in the qualitative interpretation of aeromagnetic data involves the recognition of patterns and zones with different magnetic characteristics. Three different magnetic zones were discerned based on the distinction in the intensity of the magnetic response in the total magnetic intensity (TMI)

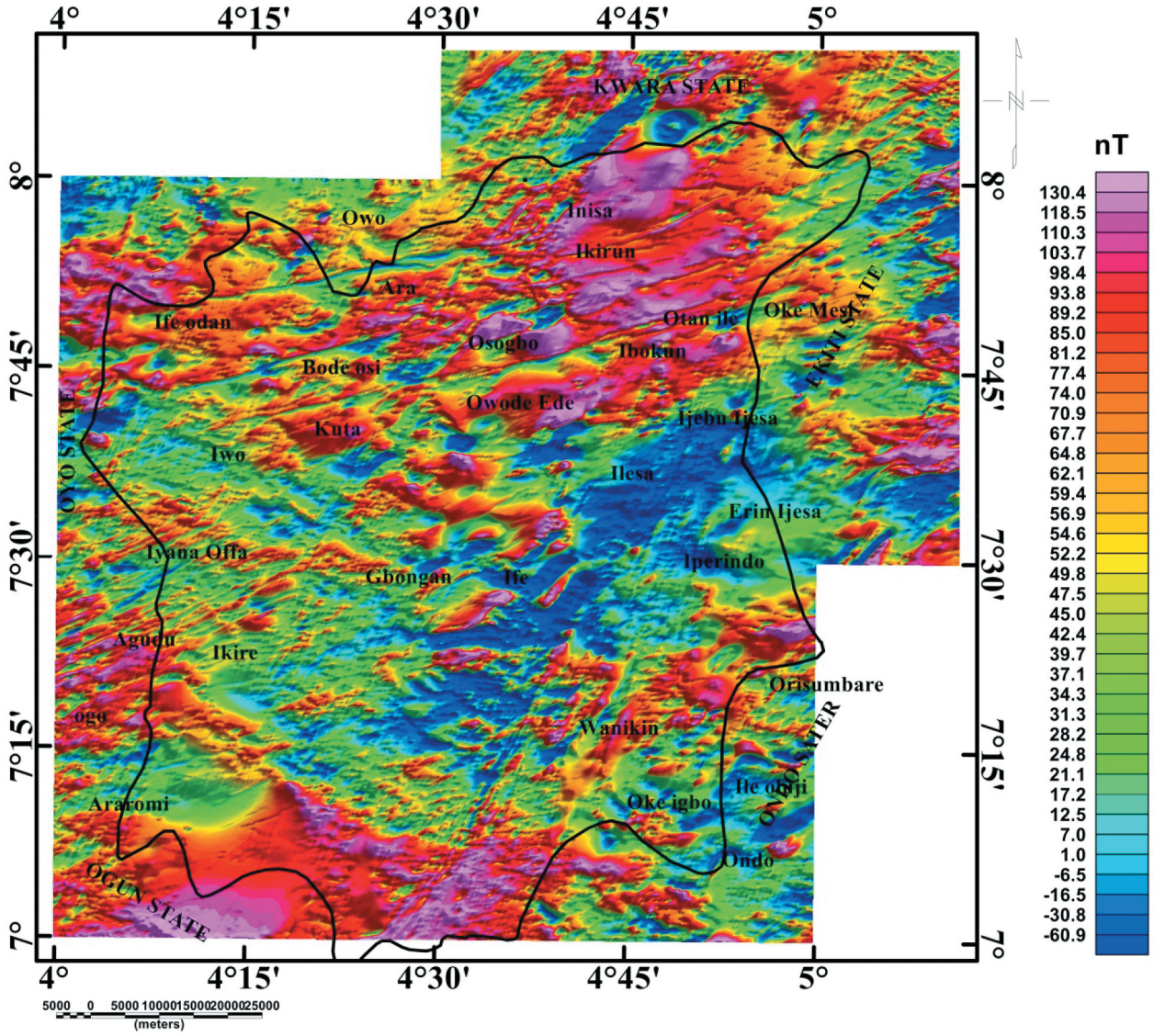

Figure 2. Continued.

map (Figure 2(a)) of the study area. These magnetic zones were assigned A, B and C. The northeastern regions of the study area assigned A (attained > 82 nT) are dominated by high amplitude magnetic anomalies, this high amplitude magnetic anomalies could be attributed to high rise basement outcrops in this region. The western regions of the study area assigned B show intermediate magnetic amplitude ranging between 14 and 78 nT while the eastern region assigned C showed low magnetic amplitude (< 9.4 nT) typical of weakly magnetised felsic rocks. This relatively low magnetic amplitude is observed in Iperindo, Erin Ijesa, Ilesa area. Furthermore, a prominent low magnetic amplitude anomaly trending NE-SW direction with magnetic intensities ranging from −77.7 to 4.1 nT is observed in the TMI map.

The reduced to the equator (RTE) map (Figure 2 (b)) showed magnetic anomalies slightly different from the TMI map (Figure 2(b)). The minimum magnetic amplitude of the anomalies in the reduced to the equator map has decreased to – 60.9 nT while the maximum magnetic amplitude value has increased to 130.4 nT. In the RTE map, magnetic low anomalies were observed within high magnetic relief zones at different parts of the study area, these magnetic lows are characteristic of rocks with relatively higher magnetic susceptibility in low magnetic latitude regions like the study area (Akinlalu et al. 2018).

Figures 3(a,b) show the HGM and ASM map of the enhanced RTE map of Osun State, respectively. The HGM map has a maximum magnetic gradient of 0.2196 nT/m. The amplitude peaks reveal the major differences in the magnetisation and correspond to a geologic contact region with differing magnetic susceptibility in the study area. The analytic signal map (Figure 3(b)) displayed three distinct magnetic zones. The low to a fairly low magnetic region with a gradient 0.0094–0.0206 nT/m is

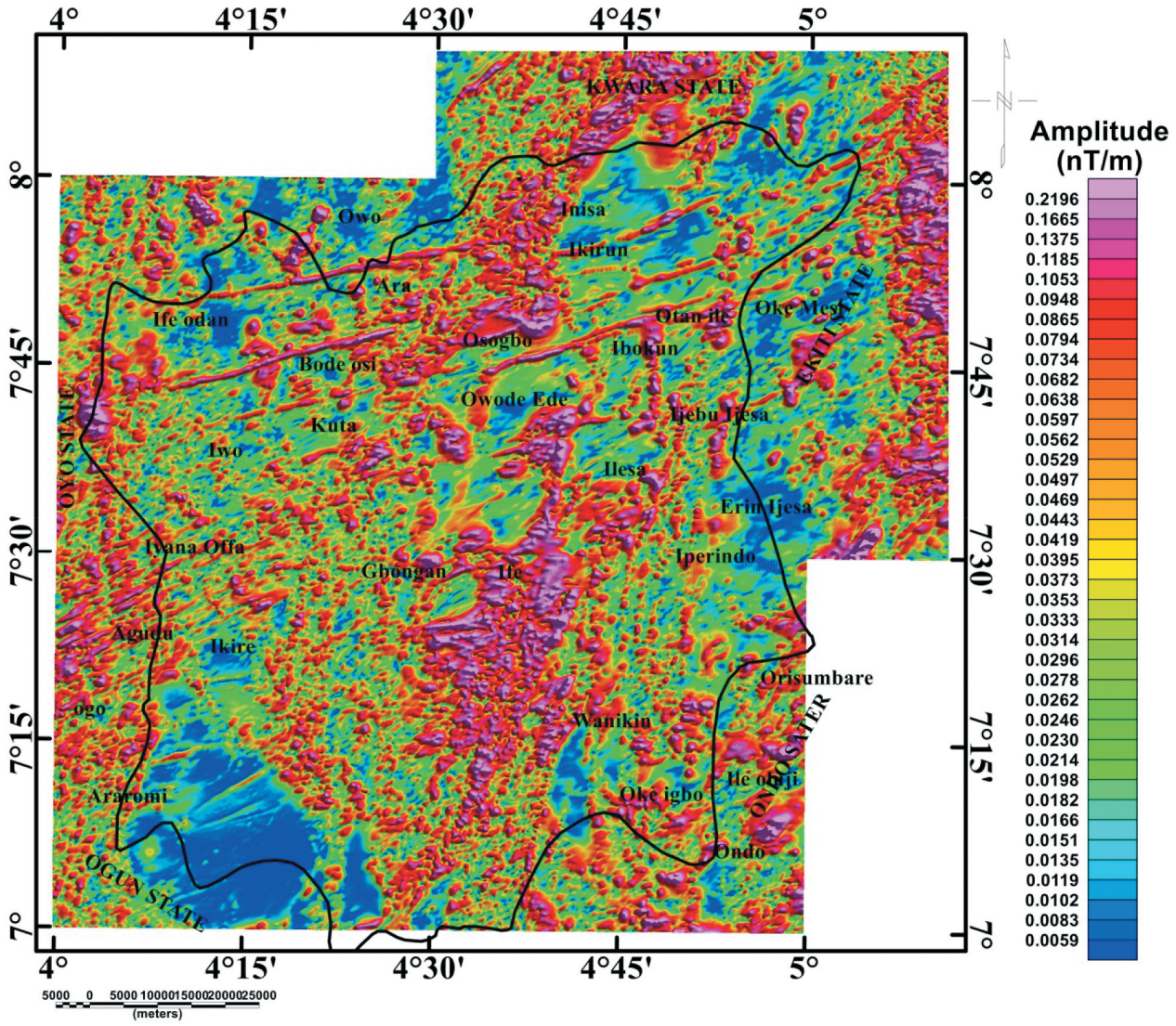

Figure 3. (a) Horizontal gradient magnitude map of Osun State.

associated with metasediments and granite because these rocks contain more quartz. The moderate zone with gradient 0.0217–0.0444 nT/m is related to granite – gneiss as these rocks contain high ferromagnesian with a low amount of felsic minerals. The zone of high magnetic anomalies zones is predominant around Ibokun, Ife, and Osogbo with intensity values of 0.0465–0.1280 nT/m are associated with ophiolitic metagabbro and gabbroic rocks, as these rocks have high ferromagnesian with an enormous amount of felsic minerals.

Figure 4 shows a well-clustered solution and depths of contacts in the area as obtained from Euler deconvolution with a structural index (SI) of zero. Reid et al. (1990) opined that a well-clustered solution reflects the suitability of the SI used. Euler solutions in the central and northeastern zones of the study area show a depth ranges of 188–260 m for the possible causative sources. In the southern region, the solutions are located at a deep depth of about 260 to 350 m. Also, in the northwestern and southeastern regions, Euler plots show non-uniform depth distribution from shallow to deep depths.

4.2. Magnetic contacts interpretation

The magnetic lineament extracted from the maxima of HGM, peaks of ASM, and an Euler solution of the study area is presented in Figure 5. The lineaments were classified into different groups based on azimuthal frequency. The set of lineaments trending NE-SW direction is the most conspicuous, corresponding to the Pan-African orogeny. The lineament delineated around Ife-Odan, Iragberi, Ikire, Ikirun, Osun, Ibokun, Iperindo among other trends in this direction. The NE-SW direction is one of the main fault orientations in the southwest basement terrain of Nigeria. Another predominant set of magnetic lineaments has a direction of NNE-SSW, Ifewara fault trend in this direction. Ifewara fault exists in the Okemesi Fold Belt, a distinguished manifestation of late-Precambrian deformation in Nigeria. Adepelumi et al. (2008) reveal

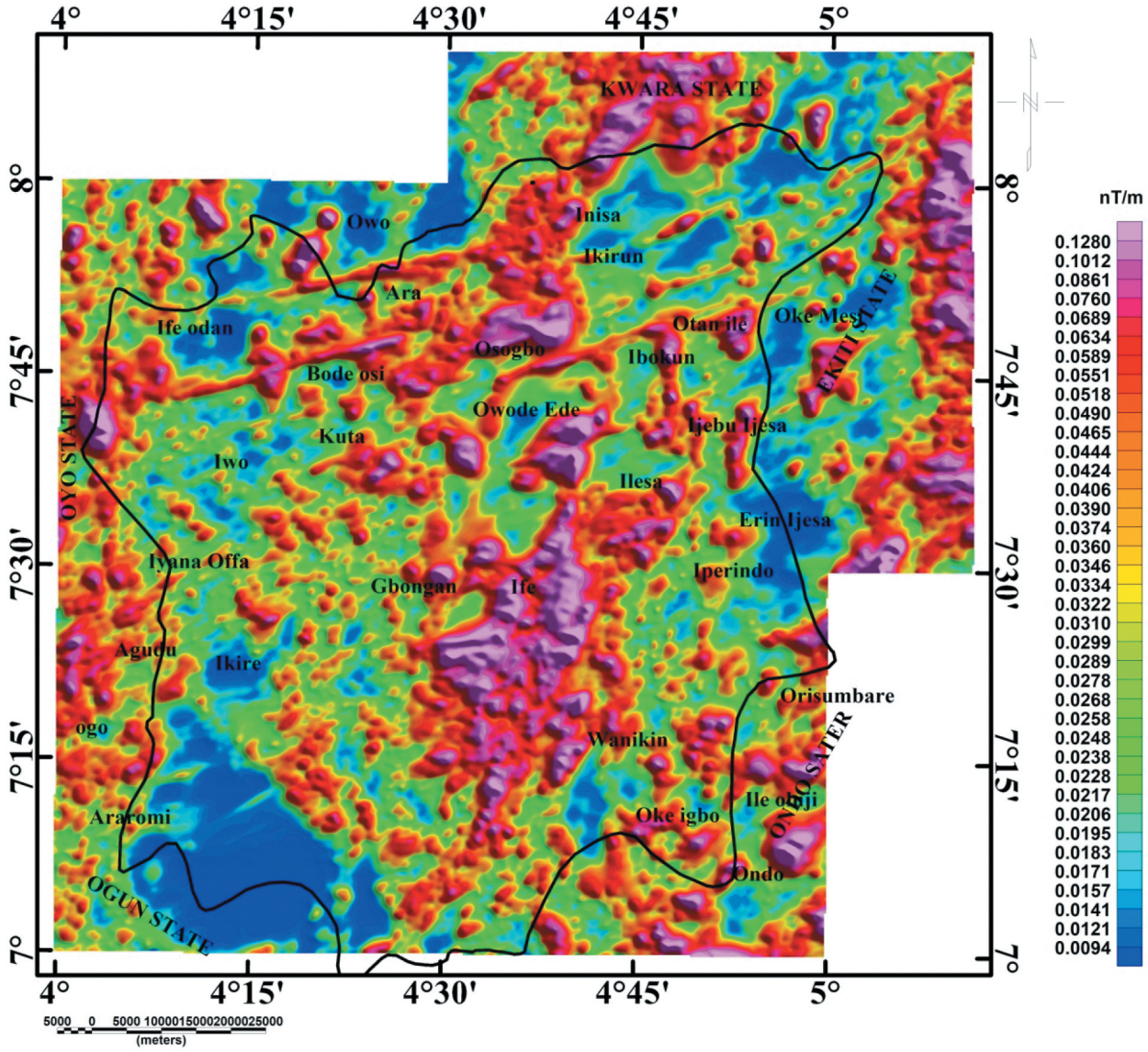

Figure 3. (b) Analytic signal magnitude map of Osun State.

the existence of Ifewara fault as a near-vertical fault trending NNE–SSW direction. Some lineaments display E-W and NW-SE trends which are probably relics of the effects of the kibaran and Liberian orogenic (Odeyemi 1988). However, two mega lineaments designated as A and B (Figure 5) detected in the analysis were previously unmapped and these features could be tectonic contacts or faults.

4.3. Surface lineament interpretation

Figure 6 reveals the ASTER DEM lineament map delineated from shaded relief image using illumination angle of 180°, 225°, 270°, 360° with sun angle of 30°. An overview by Solomon 2003; Sander 2007; Mallast et al. 2011 on the various criteria used for expulsion of morphological features in a multispectral image is used in this study. These include using auxiliary information such as hydrological (surface drainage) and topography/geology. The length of the lineaments ranged from approximately 2.8 to 27.6 km, the mean length of the identified lineaments is 5.7 km. The strike directions of the delineated lineaments as illustrated in the rose diagram are NE-SW, NNE-SSW, ENE-WSW, N-S, E-W, and NW-SE directions. The NE-SW, NNE-SSW and ENE-WSW lineaments set are the most frequent and conspicuous in the study area.

Figure 7 reveals the lineaments delineated from the mosaicked Landsat ETM+ of the investigated area after the expulsion of the morphological features. The length of the lineaments ranged from approximately 2.3 to 19.1 km, the average length of the identified lineaments is 10.7 km. The lineament directions plotted as rose diagram demonstrate the predominant directions of the lineaments are NE-SW, NNE-SSW and ENE-WSW. The NE-SW orientation is congruous with the major structural trend of the basement complex of Nigeria.

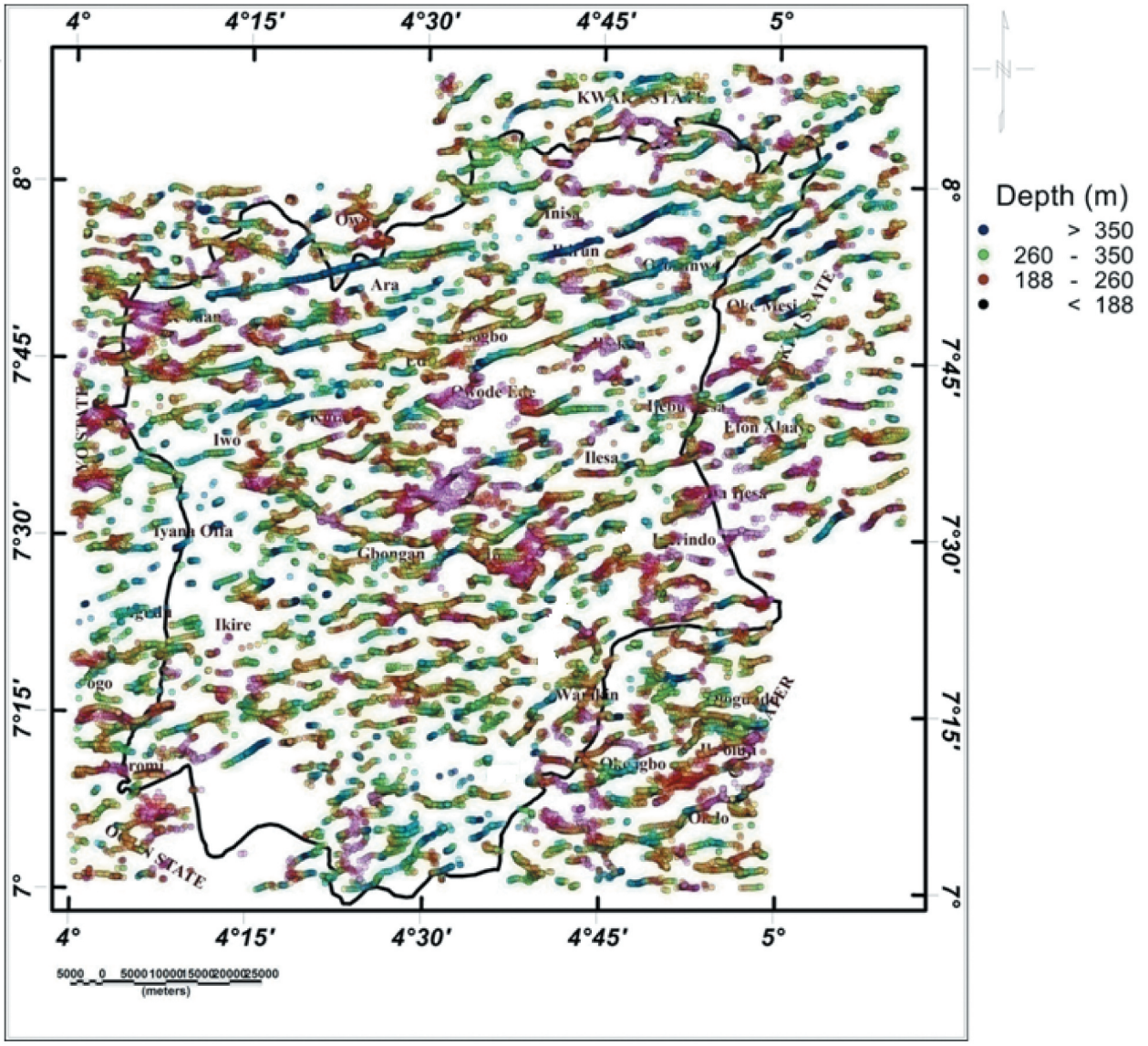

Figure 4. Euler solution map for a structural index N = 0.0 for Osun State.

Table 1. Parameters used in LINE module.

LINE Algorithm Parameter	Values (Landsat EMT +)	Values (DEM)
Filter Radius	4	12
Edge Gradient Threshold	2	80
Curve Length Threshold	2	30
Line Fitting Error Threshold	5	10
Angular Difference Threshold	10	30
Linking Distance Threshold	5	15

4.4. Composite surface tectonic lineaments

Lineaments mapped from DEM and Landsat ETM+ have spatial varieties in length, frequency and pattern. The distinctions in spatial resolution of the datasets are ascribed to the variations in the frequency of occurrence and the length of the lineaments. To derive a complete and complementary surface lineament map, the two surface tectonic lineament maps were combined. The lineaments from the two data sources (Figure 8) are congruent in many places and show broad concentrated continuous parallel zones, despite differences in spatial resolution. The major structural trends delineated in the composite surface lineament map are the NE-SW, NNE-SSW and ENE-WSW directions.

4.5. Magnetic modelling

In this study, 2.5D forward modelling was carried out to confirm the existence of some of the inferred faults as well as to quantify the changes in magnetic properties with depth and to make a plausible geologic basement surface. Four profiles were selected and modelled (Figure 5) using the Winglink software algorithm. The modelling procedure started by modifying the values of susceptibility for each basement block to decrease the variation between the observed and calculated magnetic anomaly data.

Figure 9 shows the magnetic profile, the 2.5D magnetic model, and the magnetic susceptibility of the

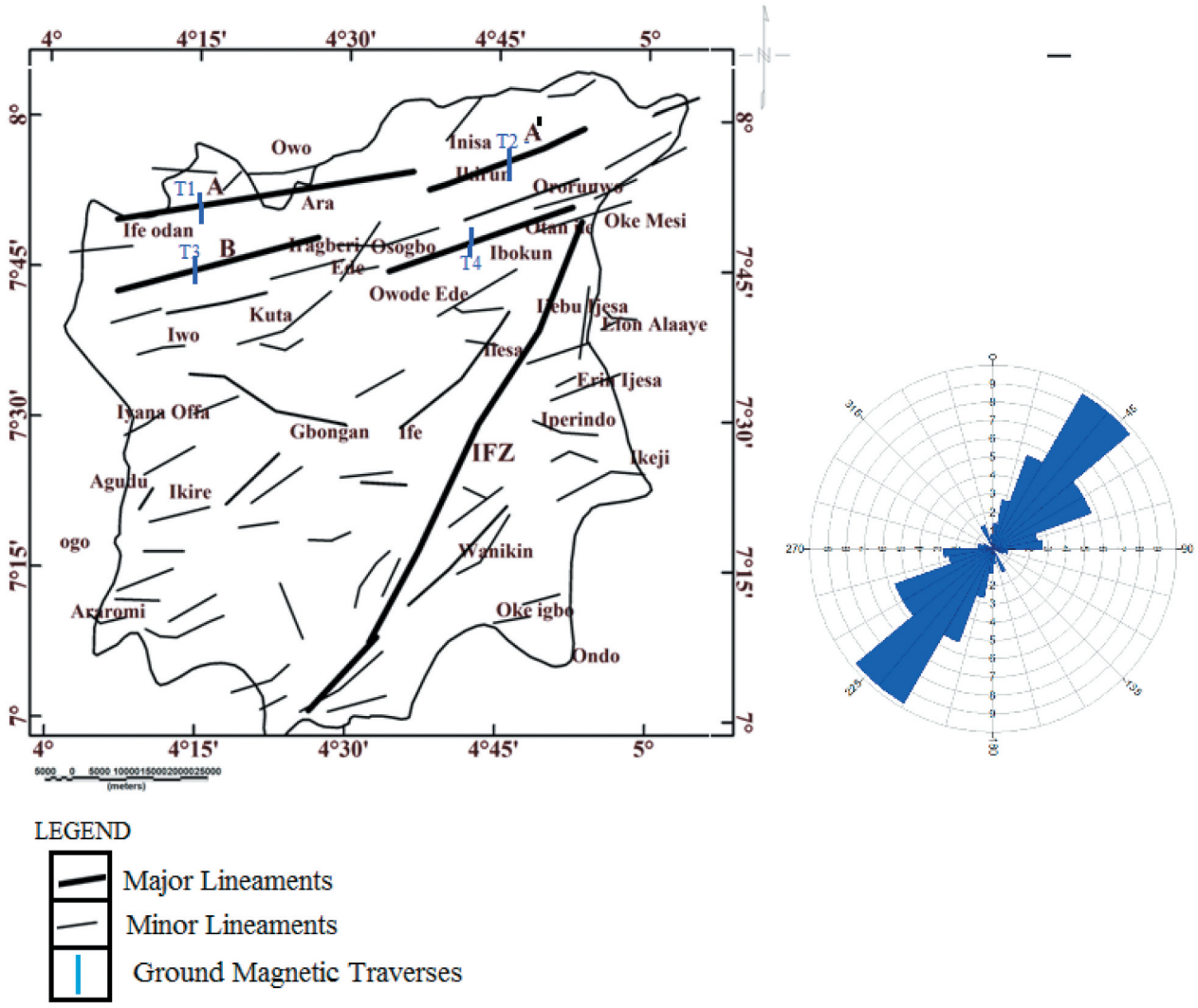

Figure 5. Inferred magnetic lineaments map of Osun State and its frequency rose diagram.

interpreted bodies along the N-S direction. The profile passes across the NW – SE lineament designated A at Ife-Odan, the upper northeastern region of the study area. The magnetic intensities range from – 205 to 180 nT (Figure 9(a)). Three recognisable trends are delineated on the magnetic profile, the northern low (stations 0–300 m), followed by a broad plateau-like low anomaly (- 205 nT) with a V-shaped, typical of a thin dyke between distance 700 and 828 m, and a gentle rise towards the south which is slightly higher than those of stations 0–300 m. The 2.5D model (Figure 9(b)), generated from the magnetic profile reveals variable magnetic basement relief. The model shows an excellent fit between the observed and calculated anomalies. Three model bodies are involved in the computation and these include the sediment (s = 0), the basement rock (s = 0.024), and the intrusion. A minor magnetic anomaly is observed between distances of 0–250 m attributed to the topography difference of the magnetic basement. The distinct and broad negative peak anomaly (v-shaped) shows a distinguished magnetic response typical of an occurrence of a thin dyke with a depth of 70 m and a lateral extent of over 100 m. The ground surface manifestation of this magnetic feature with a centre at around station distance 764 m correlates remarkably with the centre of the strike-slip fault delineated on the high-resolution magnetic data. The location of faults also matches the magnetic discontinuity surface. The magnetic susceptibility within the magnetic anomaly zone is lower than the surrounding areas.

Figure 10 reveals the magnetic profile, the 2.5D magnetic model, and the magnetic susceptibility of the interpreted bodies, the model cuts across the NW – SE lineament at the upper northern part (Ikirun) of the study area. The magnetic profile (Figure 10(a)) shows a single negative peak (with minimum amplitude of – 305 nT) between distance 1387 and 1486 m, this anomaly is surmised to be due to a geologic structure (faulted basement). The 2.5D model (Figure 10(b)), generated from the magnetic profile shows a fairly good fit between the observed and the calculated anomalies. The model bodies involved in the computation are the sediment (s = 0), basement rock (s = 0.023). The profile shows magnetic anomaly characteristic of a steeply dipping thin dyke

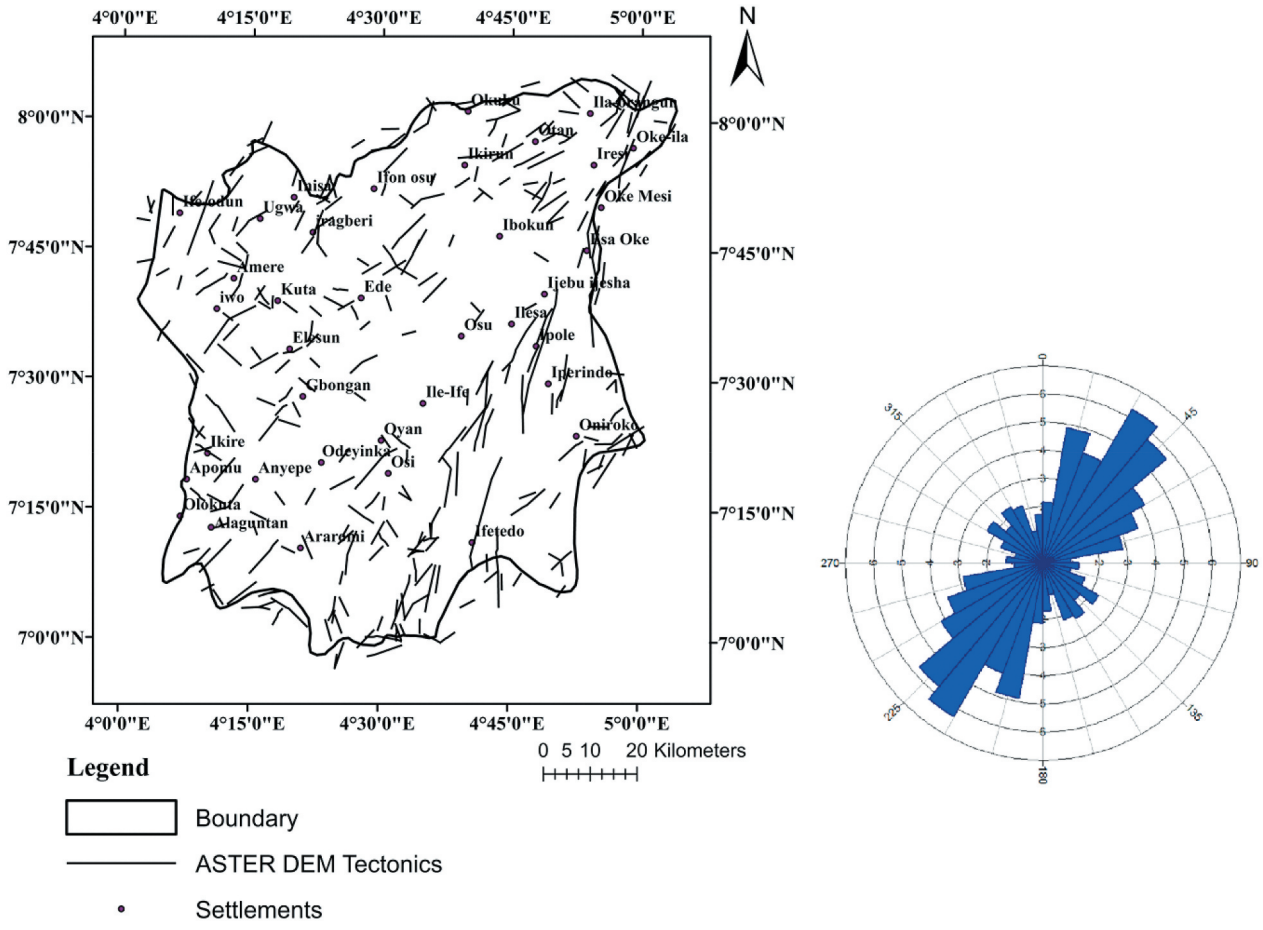

Figure 6. Tectonic lineaments obtained from ASTER DEM of Osun State and its frequency rose diagram.

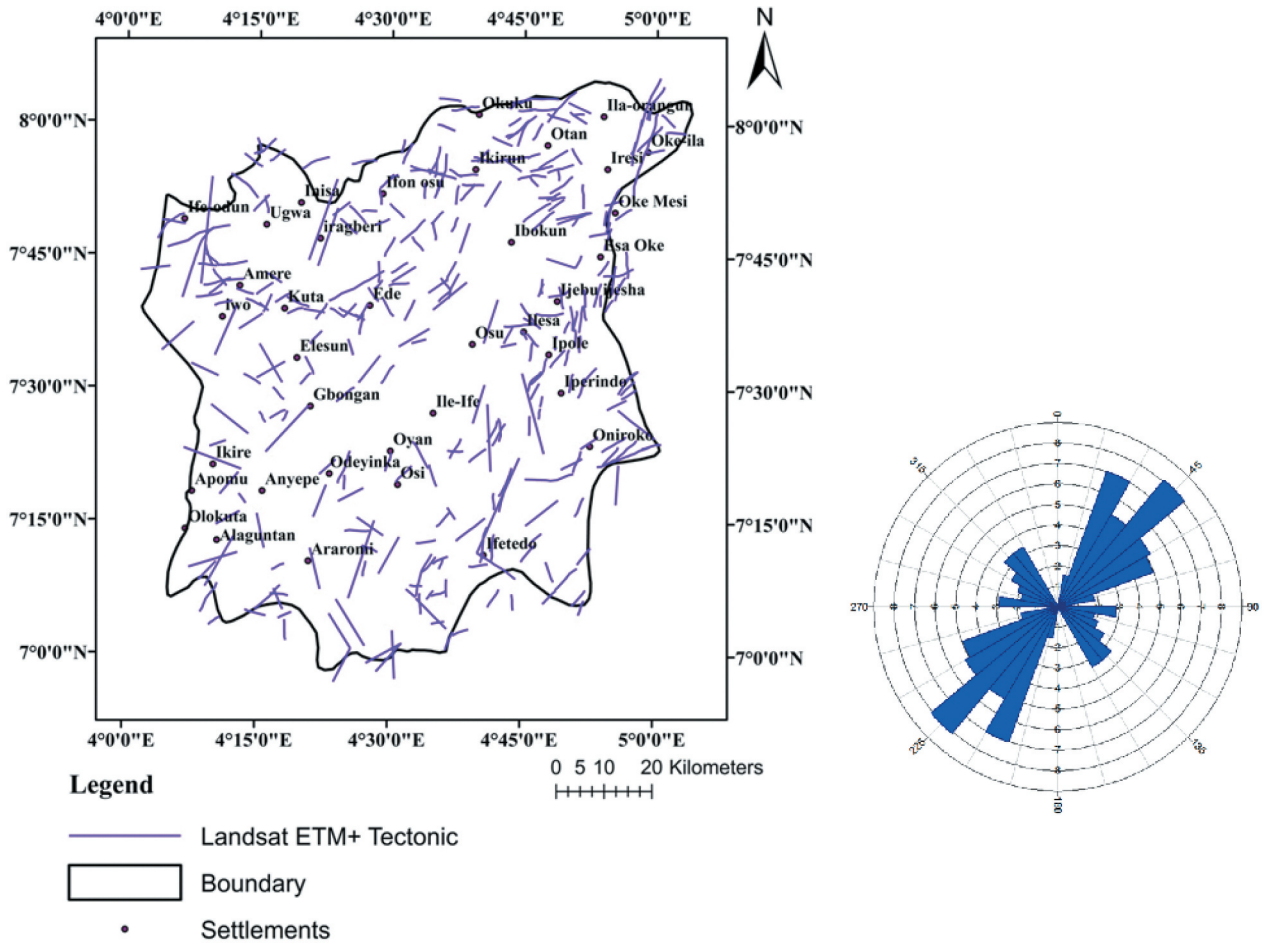

Figure 7. Tectonic lineaments obtained from Landsat EMT+ of Osun State and its frequency rose diagram.

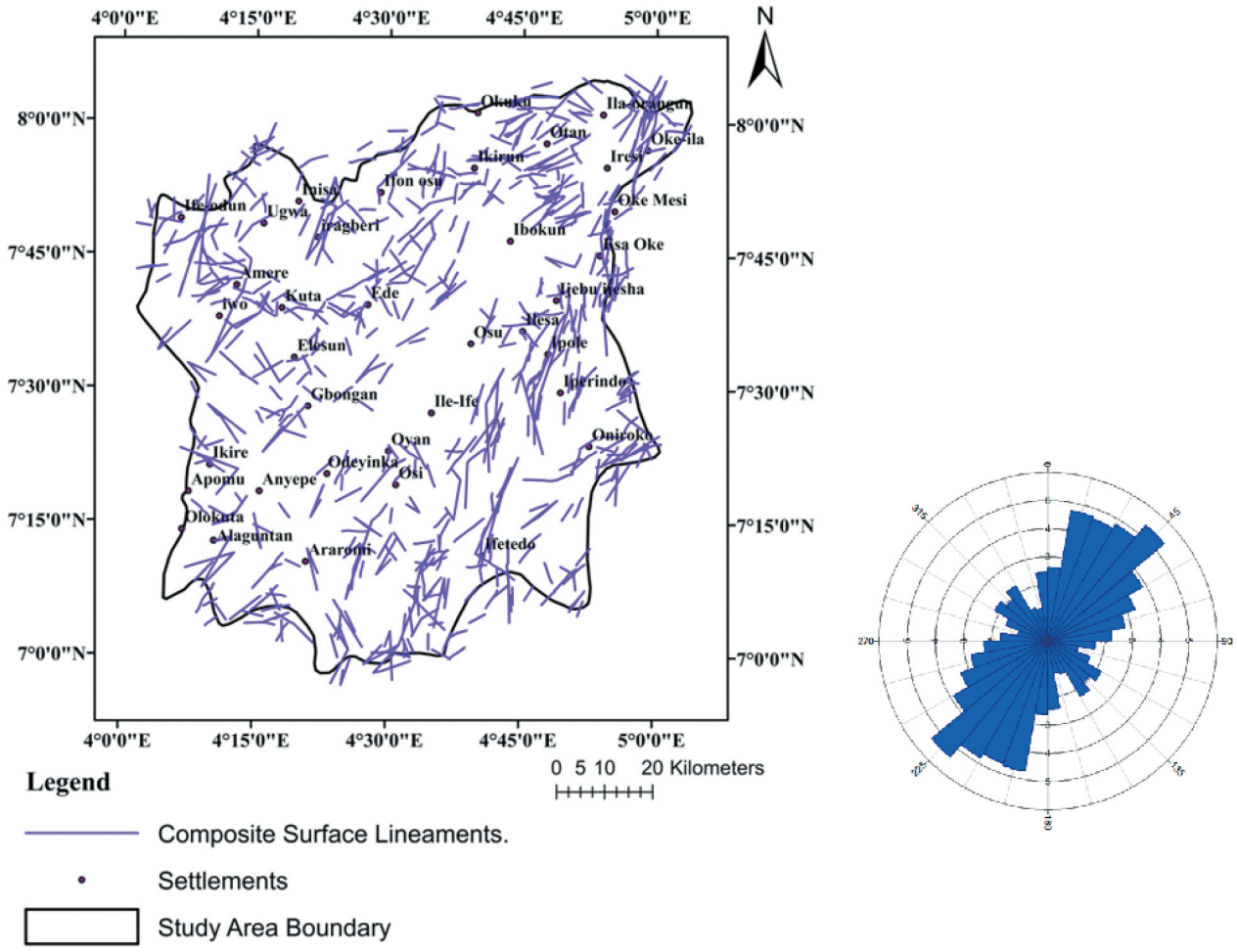

Figure 8. Composite surface tectonic lineament map of Osun State and its frequency rose diagram.

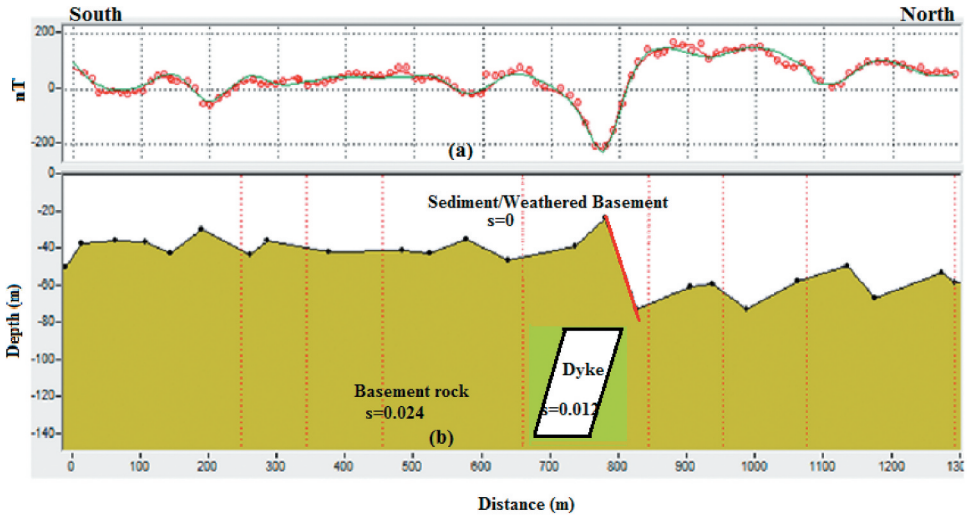

Figure 9. Geological model along profile T1 (Top – Magnetic anomaly, Bottom – Depth section).

suspected to be a fault /shear zone between stations distance 1400–1600 m with susceptibility of 0.012 SI units at a depth of 150 m, the lateral extent of the anomaly is 130 m. The ground surface manifestation of the anomaly with the centre at 1500 m correlates remarkably with the centre of the strike-slip fault delineated on the high-resolution magnetic data.

Figure 11 shows the magnetic profile, the 2.5D magnetic model, and the magnetic susceptibility of the interpreted bodies across the NW – SE lineament at the upper northeastern (Amere) part of the study area. An anomaly with a negative peak (– 600 nT) is seen between distances 200 and 300 m. The symmetry of this major anomaly depicts a steeply dipping

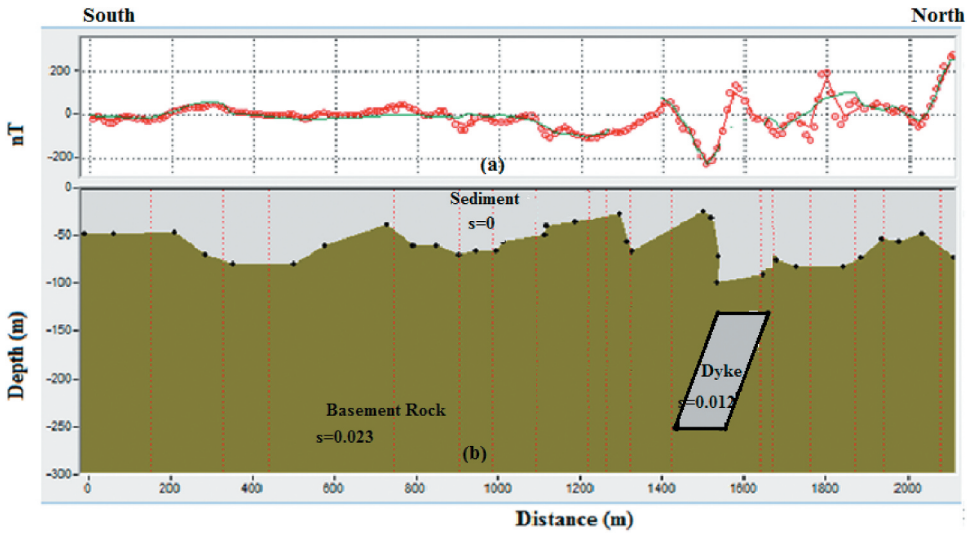

Figure 10. Geological model along profile T2 (Top – Magnetic anomaly, Bottom – Depth section).

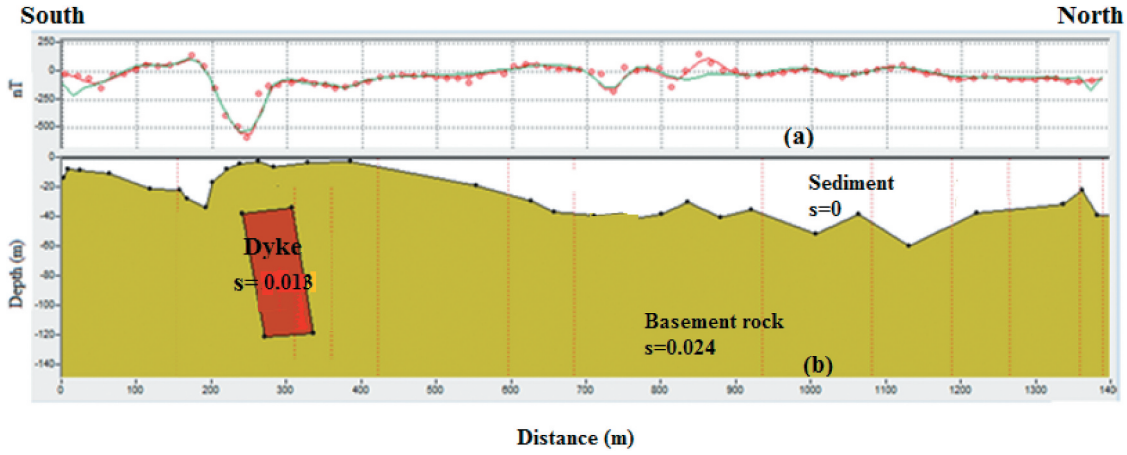

Figure 11. Geological model along profile T3 (Top – Magnetic anomaly, Bottom – Depth section).

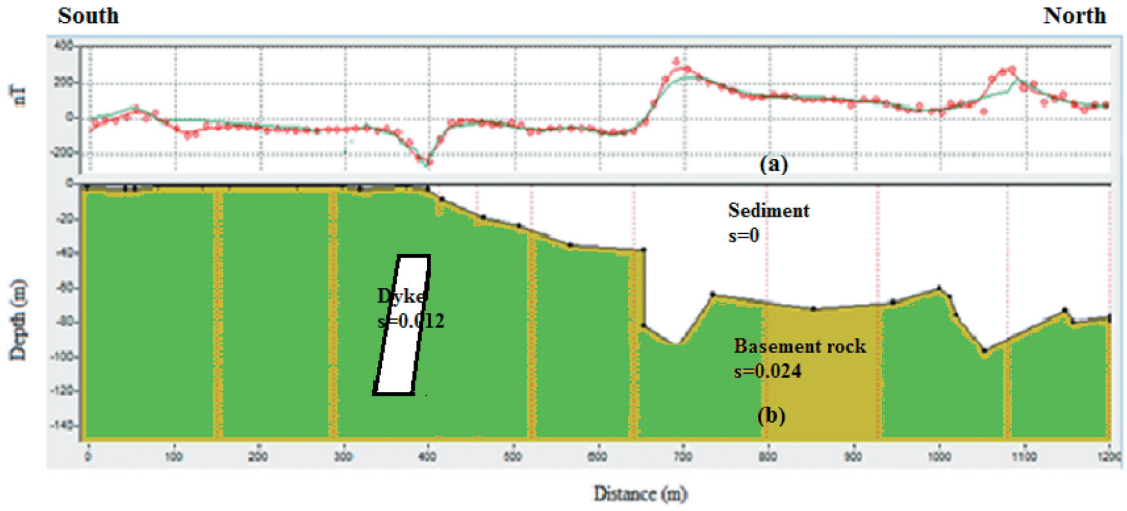

Figure 12. Geological model along profile T4 (Top – Magnetic anomaly, Bottom – Depth section).

causative body zone. The 2.5D model (Figure 11(b)), generated from the magnetic profile shows a good fit between the observed and the calculated curve. The 2.5D model shows thick overburden and relatively gentle topography. The model bodies involved in the computation are the sediment (s = 0) and the basement rock (s = 0.024). The most notable feature in the model is the low magnetic amplitudes anomaly typical

of a steeply dipping thin dyke suspected to be a fault / shear zone between stations distances 200–350 m with susceptibility of 0.013 SI at a depth of 40 m, the lateral extent of the anomaly is 50 m. The location of this anomaly is observed as a faulted zone perpendicular to the selected profile on the high-resolution magnetic survey.

Figure 12 shows the magnetic profile, the 2.5D magnetic model, and the magnetic susceptibility of the interpreted bodies across the NW – SE lineament at the upper northeastern part (Ibokun) of the study area. The magnetic profile (Figure 12(a)) shows a single negative peak (- 230 nT) amplitudes between 430 and 468 m. The 2.5D model (Figure 12(b)), generated from the magnetic profile displays an uneven magnetic basement relief. The modelled profile shows an excellent fit between the calculated and the observed curve. The model bodies involved in the computation are the sediment (s = 0) and basement rock (s = 0.024). The most striking feature of this model is the v-shaped anomaly which shows a prominent magnetic response typical of an occurrence of a thin dyke with susceptibility of 0.012 SI at a depth of 30 m having a lateral extent of 20 m. The magnetic field minima (negative anomalies) are associated with structural lows and down-faulted blocks.

5. Conclusion

In this study, airborne magnetic data, DEM and Landsat 7 ETM + were used to delineate surface and subsurface structural lineaments in Osun State, Southwestern, Nigeria. Mapping of surface and subsurface lineaments was performed on satellite images (Landsat ETM+ and DEM) and airborne magnetic datasets, respectively. The application of selected enhancement methods (HGM, ASM, and 3-D Euler Deconvolution) on the magnetic data shows the subsurface structural element in the study area. The structural map (magnetic lineaments) revealed many discontinuity zones in a different orientation in the study area indicating a complex tectonic history and several events of deformation. The magnetic lineaments show that the area has been exposed to significant regional field stress. The structural trends of the composite lineament map show predominant lineament directions; NE-SW, NNE-SSW, E-W, and NW-SE. These trends were in agreement with the major regional tectonic trends of Southwestern Nigeria. The conspicuous NE-SW pattern may have an affinity with the major basement lineaments and faults that were created during the Pan-African consolidation. Two mega lineaments detected in the analysis were previously unmapped and these features were mapped as a thin dyke. The satellite imageries (Landsat ETM+ and DEM) depict a characteristics feature of the occurrence of underlying structures in the basement complex of Osun State. The major lineaments trends delineated in the composite surface lineament map are the NE-SW, NNE-SSW, and ENE-WSW directions. The integrated techniques allowed the extraction of valuable structural mapping otherwise difficult by conventional field mapping. The 2.5-D model revealed several peaks, indicating the locations of shallow magnetic structures underlying the area of highest magnetisation. These model profiles show a good fit between the regional magnetic curve and the theoretical one which confirms and indicates that the proposed basement relief, where the magnetic field maxima and minima express the effect of structural highs and structural lows, respectively. The depth to the top of the basement across these peaks ranges from zero (outcropping) to 100 m. The integrated techniques allowed the extraction of valuable structural mapping otherwise difficult by conventional field mapping. The derived lineaments provide essential support for early stages of mineral prospecting and can serve as a reference for future geological and structural mapping.

Disclosure statement

No potential conflict of interest was reported by the author(s).

Funding

No funding is available for this work.

ORCID

Adebiyi S. Adebayo http://orcid.org/0000-0001-6152-0569
Oluwaseyi A. Dasho http://orcid.org/0000-0001-8514-0181

References

Adebayo AS. 2018. Investigation of spatial relationship between magnetic and remote sensing derived lineaments and mineralization in the basement complex terrain of Osun State, Nigeria [P.hD. Thesis]. Ile-Ife (Nigeria): Obafemi Awolowo University.

Adepelumi AA, Ako BD, Ajayi TR, Olorunfemi AO, Awoyemi MO, Falebita DE. 2008. Integrated geophysical mapping of the Ifewara transcurrent fault system, Nigeria. J Afr Earth Sci. 52:161–166. doi:10.1016/j.jafrearsci.2008.07.002.

Adetoyinbo AA, Bello AK, Hammed SO. 2010. The geological and geochemical characteristics of the soil on ore deposits-Itagunmodi gold deposits as a case study. J Min Geol. 11:55–70.

Akinlalu AA, Adelusi AO, Olayanju GM, Adiat KAN, Omosuyi GO, Anifowose AYB, Akeredolu BE. 2018. Airborne magnetic mapping of basement structures and mineralization characterization of Ilesa Schist Belt, Southwestern Nigeria. J Afr Earth Sci. 138:383–391. doi:10.1016/j.jafrearsci.2017.11.033.

Bahiru EA, Woldai T. 2016. Integrated geological mapping approach and gold mineralization in Buhweju area, Uganda. Ore Geol Rev. 72:777–793. doi:10.1016/j.oregeorev.2015.09.010.

Boucher RK. 1995. The relevance of lineament tectonics to hydrocarbon occurrences in the Cooper and Eromanga Basins, South Australia. J Pet Explor Soc Aust. 21:69–75.

Briggs IC. 1974. Machine contouring using minimum curvature. Geophysics. 39:39–48. doi:10.1190/1.1440410.

Dasho OA, Ariyibi EA, Akinluyi FO, Awoyemi MO, Adebayo AS. 2017. Application of satellite remote sensing to groundwater potential modeling in Ejigbo area, Southwestern Nigeria. Model Earth Syst Environ. 3:615–633. doi:10.1007/s40808-017-0322-z.

Elhag M, Bahrawi JA. 2014. Conservational use of remote sensing techniques for a novel rainwater harvestingin arid environment. Environ Earth Sci. 72:4995–5005. doi:10.1007/s12665-014-3367-6.

Falconer JD. 1911. The geology and geography of Northern Nigeria. London: Macmillan.

Jiang YL, Zhao K, Liu JD. 2018. A quantitative method for evaluating the transporting capacity of oil-source faults in shallow formation of oil-rich sags. Acta Geol Sin (English Edition). 4:1678–1679. doi:10.1111/1755-6724.13663.

Keating P, Zerbo L. 1996. An improved technique for reduction to the pole at low latitudes. Geophysics. 61:131–137. doi:10.1190/1.1443933

MacLeod IN, Jones K, Dai TF. 1993. 3-D analytic signal in the interpretation of total magnetic field data at low magnetic latitudes. Explor Geophys. 24:679–688. doi:10.1071/EG993679.

Mallast U, Gloaguen R, Geyer S, Rodiger T, Siebert C. 2011. Semi-automatic extraction of lineaments from remote sensing data and the derivation of groundwater flow paths. Hydrol Earth Syst Sci Discuss. 8:1399–1431.

Masoud A, Koike K, Teng Y. 2007. Geothermal reservoir characterization integrating spatial GIS models of temperature, geology, and fractures. Proceedings of 12th Conference of International Association for Mathematical Geology; Aug 26–31; Beijing, China. (on CD-ROM).

Masoud AA, Koike K. 2011. Auto-detection and integration of tectonically significant lineaments from SRTM DEM and remotely-sensed geophysical data. ISPRS J Photogramm Remote Sens. 66:818–832. doi:10.1016/j.isprsjprs.2011.08.003.

Nigeria Geological Survey Agency. 2006. The geological map of Nigeria. Abuja: NGSA.

Odeyemi IB. 1988. Lithostratigraphy and structural relationships of the upper Precambrian metasediments igarra area, southwestern Nigeria. In: Oluyide PO, Mbonu WC, Ogezi AE, Egbiniwe IG, Ajibade AC, Umeji AC, editors. Precambrian Geological Survey of Nigeria; p. 111–125.

Oelkers EH, Bénézeth P, Pokrovski GS. 2009. Thermodynamic databases for water-rock interaction. Rev Mineral Geochem. 70:1–46. doi:10.2138/rmg.2009.70.1.

Olorunfemi MO, Oni AG. 2019. Integrated geophysical methods and techniques for sitting productive boreholes in basement complex terrain of Southwestern Nigeria. 13–26.

Oyeyemi KD, Aizebeokhai AP. 2018. Geoelectrical Investigations for groundwater exploration in crystalline basement terrain, SW Nigeria: implications for groundwater resources sustainability. Int J Civ Eng Technol (IJCIET). 9(6):765–772.

Phillips J. 2000. Locating magnetic contacts: a comparison of the horizontal gradient, analytic signal, and local wavenumber methods. 70th Annual International Meeting, SEG, Expanded Abstracts, 402–405

Rahaman MA. 1976. Review of the basement geology of southwestern Nigeria. In: Kogbe CA, editor. Geology of Nigeria. Lagos: Elizabethan Publishing Company; p. 41–56.

Reid AB, Allsop JM, Granser H, Millett AJ, Somerton IW. 1990. Magnetic interpretation in three dimensions using Euler deconvolution. Geophysics. 55:80–91. doi:10.1190/1.1442774.

Sander P. 2007. Lineaments in groundwater exploration: a review of applications and limitations. Hydrogeol J. 15 (1):71–74. doi:10.1007/s10040-006-0138-9.

Solomon S. 2003. Remote sensing and GIS: applications for groundwater potential assessment in eritrea [A Ph.D. Thesis Submitted to the Department of Environmental and Natural Resources Information Systems]. Sweden: Royal Institute of Technology; p. 137.

Webring M. 1981. MINC: a gridding program based on minimum curvature. US Geol Surv. 81–1224:43.

Wu KY, Qu JH, Wang HH. 2014. Strike-slip characteristics, forming mechanisms, and controlling reservoirs of Dazhuluogou fault in the Junggar Basin. J CHINA Univ Petrol. 38(5):0041–004711.